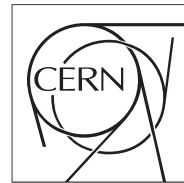




**The Compact Muon Solenoid Experiment**  
**Conference Report**

Mailing address: CMS CERN, CH-1211 GENEVA 23, Switzerland



**15 January 2025 (v2, 07 February 2025)**

# Searches in the long-lived particle and dark sectors

Daniele Trocino for the ATLAS and CMS Collaborations

## Abstract

Searches for dark matter (DM) and long-lived particles (LLPs) are a key focus of the ATLAS and CMS experiments at the Large Hadron Collider. Astrophysical evidence points to the existence of DM, but its nature remains elusive. In addition, many theories predict LLPs that leave distinctive signatures in the detectors, including displaced vertices and unusual ionization patterns. This work reviews the latest findings from ATLAS and CMS, as well as the innovative methods developed for these searches. These efforts have placed stringent constraints on several theoretical models, and opened the way for potential discoveries in the dark sector.

Presented at *Blois2024 35th Rencontres de Blois on Particle Physics and Cosmology*

## Searches in the long-lived particle and dark sectors

Daniele Trocino on behalf of the ATLAS and CMS Collaborations

*Istituto Nazionale di Fisica Nucleare, Sezione di Torino,  
Via Pietro Giuria 1, 10125 Torino, Italy*



Searches for dark matter (DM) and long-lived particles (LLPs) are a key focus of the ATLAS and CMS experiments at the Large Hadron Collider. Astrophysical evidence points to the existence of DM, but its nature remains elusive. In addition, many theories predict LLPs that leave distinctive signatures in the detectors, including displaced vertices and unusual ionization patterns. This work reviews the latest findings from ATLAS and CMS, as well as the innovative methods developed for these searches. These efforts have placed stringent constraints on several theoretical models, and opened the way for potential discoveries in the dark sector.

### 1 Introduction

Astrophysical observations strongly suggest the existence of dark matter (DM)<sup>1,2,3</sup>, constituting about 27% of the mass-energy density of the universe. Despite its abundance, the nature of DM remains unknown. Direct and indirect detection experiments have yielded tantalizing hints, but no conclusive evidence. Collider experiments like ATLAS<sup>4,5</sup> and CMS<sup>6,7</sup> aim to produce and detect DM candidates through high-energy proton-proton collisions at the Large Hadron Collider (LHC).

In parallel, many extensions of the standard model (SM) predict the existence of long-lived particles (LLPs), which could provide a window into hidden sectors of particle physics. These particles are characterized by extended lifetimes due to suppressed decay mechanisms, and their signatures include displaced vertices (DVs), tracks with non-standard ionization energy loss ( $dE/dx$ ), or delayed signals. LLPs arise in a wide variety of beyond-the-SM (BSM) scenarios, including supersymmetry (SUSY), models with exotic Higgs bosons, and theories incorporating dark sectors (DSSs).

The ATLAS and CMS experiments have developed extensive search programs for DM and LLPs<sup>8,9,10,11</sup>, leveraging advanced detector technologies. For DM, typical signatures involve missing transverse energy (MET) accompanied by visible particles, such as jets, photons, or vector bosons<sup>12</sup>. The unique experimental signatures produced by LLPs require innovative techniques, such as precise tracking for DVs and timing measurements for delayed signals or slow particles.

In the absence of significant excesses over the SM expectations, these searches have imposed stringent constraints on a wide range of models. The next sections provide an overview of the main

techniques used in the search for DSs and LLPs, and a selection of recent results from ATLAS and CMS.

## 2 Experimental signatures and detection strategies

Both the ATLAS<sup>4</sup> and CMS<sup>6</sup> apparatuses are comprised of an inner tracking detector (ID), electromagnetic and hadronic calorimeters (ECAL and HCAL), and a muon spectrometer (MS). Signals of DSs and LLPs can manifest in various ways within the detectors:

- neutral, stable particles that escape detection, recoiling against a visible system, such as jets, photons, W or Z bosons, etc. (referred to as “MET + X”);
- prompt jets with distinctive, unusual features, e.g. jets with very large radii, semi-visible jets, or flows of unclustered hadrons;
- tracks with unusual ionization levels, such as multiply or fractionally charged particles and slow, heavy particles;
- isolated tracks with large impact parameters (referred to as “displaced tracks” hereafter) and DVs formed by two or more displaced tracks;
- nonprompt jets produced within the ID (enriched in DVs) or outside the ID (jets in ECAL and HCAL, in HCAL only, or high-multiplicity hadronic showers in the MS).

## 3 MET + X searches

### 3.1 DM + top quark (“mono-top”)

ATLAS and CMS conducted searches for DM production in association with a single top quark<sup>13</sup>, analyzing approximately  $140\text{ fb}^{-1}$  of proton-proton (pp) collision data at  $\sqrt{s} = 13\text{ TeV}$ , collected during the LHC Run-2 (2015–18)<sup>14,15</sup>. The searches target top quarks with a large Lorentz boost and with fully hadronic decays, producing final states with a large-radius jet and large MET. Both experiments make use of neural network taggers to identify the top-quark jets.

CMS focused on a simplified model for DM production<sup>12</sup>, where the top quark is produced via a flavor-changing neutral current, with a hypothetical vector mediator decaying into two fermionic DM candidates. Mediator and DM masses were excluded at 95% confidence level (CL) up to 1.85 TeV and 750 GeV, respectively (see fig. 1 left). ATLAS also provided an interpretation with a scalar mediator, excluding its mass up to 4.3 TeV (see fig. 1 right).

### 3.2 DM + bottom quarks

CMS conducted the first search at the LHC for DM particles produced in association with two nonresonant bottom quarks, analyzing the full LHC Run-2 data set<sup>16</sup>. The study targets events with large MET and a pair of b-quark jets (“b-tagged” jets), using the hadronic recoil and the jet angular distributions to discriminate the signal from the abundant SM backgrounds. Results are interpreted within the framework of a type-II two-Higgs-doublet model with an additional light pseudoscalar (2HDM+ $a$ )<sup>12</sup>, achieving sensitivity to the parameter space with  $\tan\beta$  greater than 15. The mass of the lighter pseudoscalar is excluded up to 260 GeV at 95% CL.

### 3.3 DM + hadronically decaying vector bosons (“mono- $V(qq)$ ”)

Using the full LHC Run-2 data set, ATLAS analyzed events with large MET and a hadronically decaying W or Z boson, either reconstructed as two jets or as a single large-radius jet<sup>17</sup>, leveraging advanced techniques in jet substructure.

The results are interpreted in the context of several BSM models: simplified models where pairs of fermionic DM particles are produced via vector (axial-vector) mediators, excluded at 95%

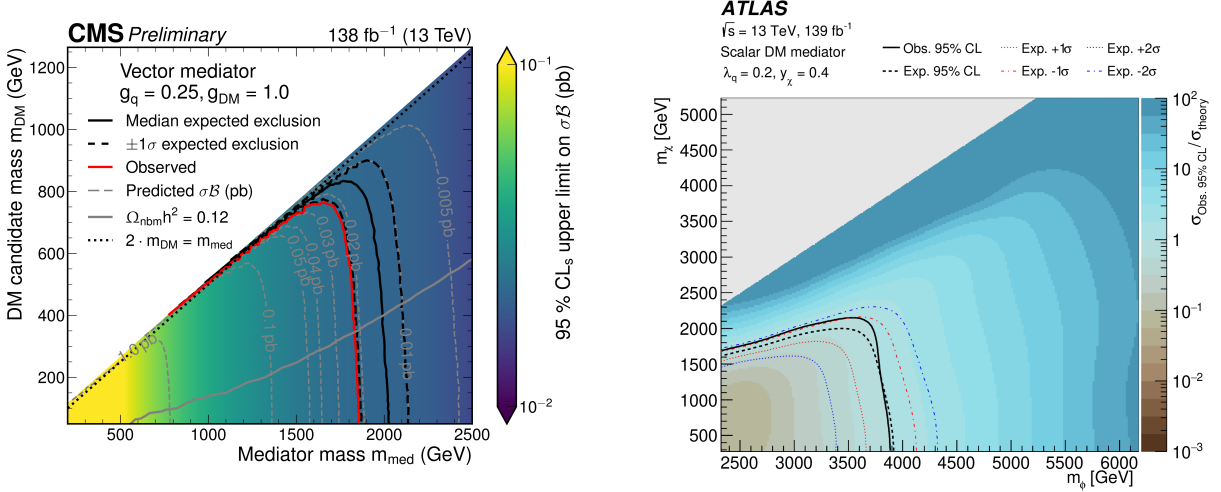


Figure 1 – Upper limits at 95% CL on the DM production cross section times branching ratio (or cross section divided by the theoretical value) from the mono-top searches, as a function of the mediator and DM masses. Left: CMS search with a vector mediator; right: ATLAS search with a scalar mediator.

CL for masses up to 955 (965) GeV; 2HDM+ $a$  models, placing limits on the masses of the two pseudo-scalar bosons  $a$  and  $A$ ; “invisible Higgs” models where the 125 GeV Higgs boson decays to DM candidates<sup>18,19</sup>, setting an upper limit on the invisible branching fraction of 0.34; and axion-like particle (ALP) production in association with a W or Z boson<sup>20</sup>. Model-independent limits are also established, with visible cross sections for BSM processes excluded for different MET thresholds used in the signal selection.

### 3.4 Invisible Higgs searches

In “Higgs-portal” models<sup>12,18,19</sup>, the Higgs boson acts as a mediator coupling the SM particles to invisible states in a hypothetical DS, such as DM candidates or LLPs that escape the detector without interacting. The branching ratio of the Higgs boson to invisible states in the SM is  $B_{\text{inv}} \simeq 10^{-3}$ , solely due to the decay into four neutrinos. A higher  $B_{\text{inv}}$  value would be a definitive signature of BSM physics.

ATLAS and CMS target invisible Higgs decays using several production modes<sup>21,22</sup>: vector boson fusion (VBF), associated production with a W or Z boson (VH), or gluon-gluon fusion (ggF). The statistical combination of all these searches conducted with LHC Run-1 ( $\sqrt{s} = 7\text{--}8$  TeV, 2010–12) and Run-2 data allows ATLAS and CMS to place upper limits on  $B_{\text{inv}}$  as low as 0.107 (see fig. 2 left), exceeding the indirect limits derived from the measurements of the SM Higgs couplings<sup>23</sup>. The observed limits on  $B_{\text{inv}}$  are also translated into limits on the DM-nucleon scattering cross section and compared to results from direct-detection experiments, proving complementary for DM masses below 10–20 GeV (see fig. 2 right).

## 4 Prompt, visible signatures

### 4.1 Dark meson searches

Dark mesons  $\pi_D$  and  $\rho_D$  arise as bound states of a hypothetical  $SU(2)$  “dark QCD”<sup>24</sup>. Under certain conditions (e.g., for a  $\pi_D$ -to- $\rho_D$  mass ratio  $\eta_D < 0.5$ ),  $\rho_D$  decays predominantly to  $\pi_D$  pairs, and  $\pi_D$  to SM top and bottom quarks.

ATLAS conducted a search for such dark mesons decaying into top and bottom quarks<sup>25</sup>, utilizing the full Run-2 data set. The search focuses on fully hadronic final states, as well as final states with exactly one electron or muon accompanied by multiple jets. The selection requires 5

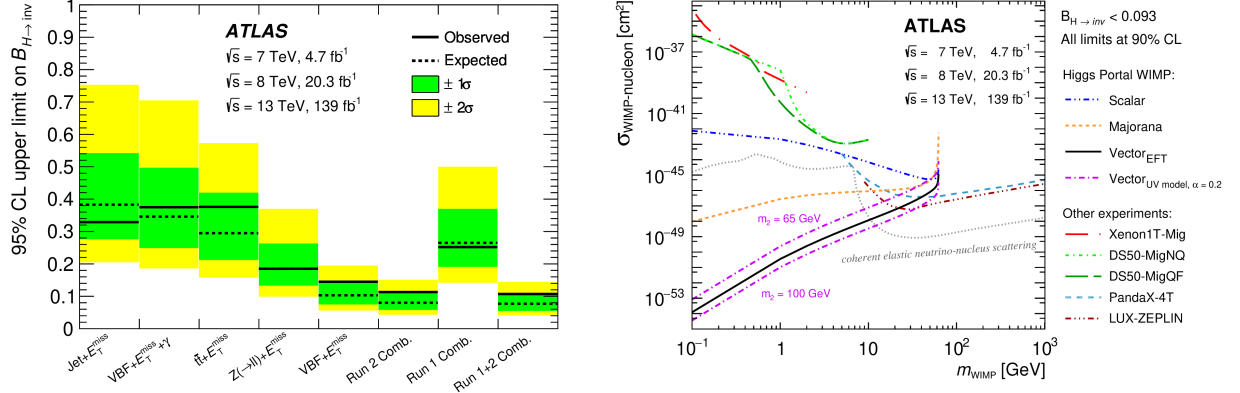


Figure 2 – Left: upper limits at 95% CL on  $B_{\text{inv}}$  for all the ATLAS Run-2 invisible-Higgs searches and their combination. Right: upper limit at 90% CL on the spin-independent DM-nucleon scattering cross section as a function of the DM mass for a selection of direct detection experiments, compared with the interpretation of the ATLAS combined limit on  $B_{\text{inv}}$  in the context of Higgs portal models.

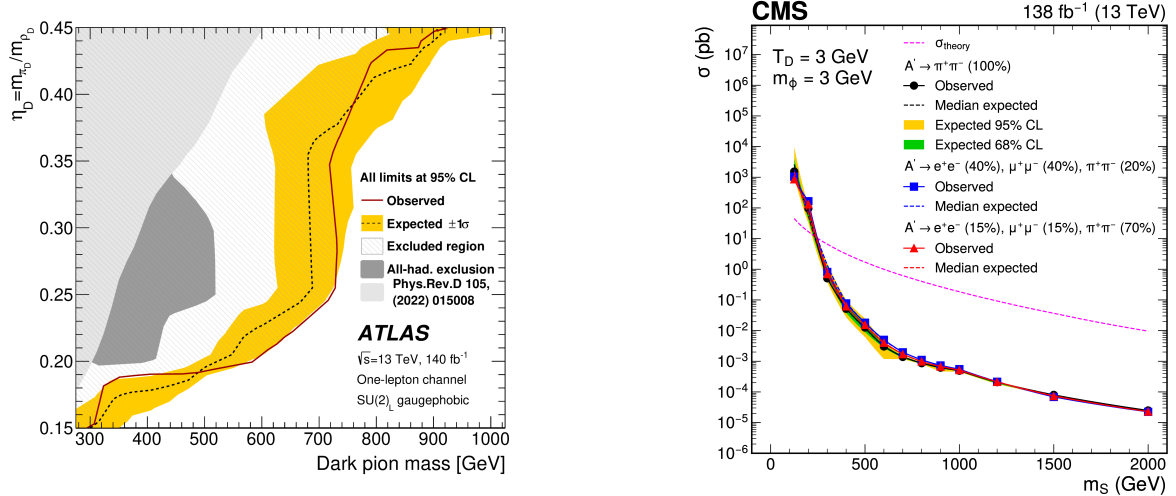


Figure 3 – Left: exclusion contours at 95% CL in the  $\eta_D$ - $\rho_D$  mass plane for the ATLAS dark meson search, in the fully hadronic (grey area) and one-lepton (red line) channels. Right: 95% CL exclusion limits on the SUEP production cross section for the CMS search, as a function of the scalar mediator mass.

or 6 jets in a boosted topology (i.e., reclustered into two large-radius jets), three of which must be  $b$ -tagged.

The analysis sets exclusion limits on the  $\pi_D$  and  $\rho_D$  masses (see fig. 3 left). For  $\eta_D = 0.45$  (0.25), dark pions with masses below 940 (740) GeV are excluded at the 95% CL.

#### 4.2 Search for soft unclustered energy patterns

“Soft unclustered energy patterns” (SUEPs) arise in dark QCD models featuring a confining force with a large ’t Hooft coupling<sup>26</sup>. SUEPs could be produced in LHC collisions, leading to final states characterized by numerous low-momentum, isotropically distributed particles.

CMS conducted the first dedicated search for SUEPs<sup>27</sup>, using the full LHC Run-2 data set. This analysis targets events with boosted topologies, where a SUEP recoils against a high-momentum jet from initial state radiation. The signal selection requires two large-radius track clusters, with the higher-multiplicity one being identified as the SUEP candidate. The multiplicity and sphericity of the clustered tracks are employed to suppress SM multi-jet backgrounds. The search set upper limits on the production cross section via gluon fusion of a scalar mediator decaying into SUEP-like final states (see fig. 3 right).

### 4.3 Search for fractionally charged particles

Fractionally charged particles (FCPs), which have electric charges less than that of the electron ( $e$ ), are hypothesized in various BSM theories<sup>28</sup>. CMS carried out a search for FCPs in the full Run-2 LHC data set<sup>29</sup>. The analysis aims to identify FCPs through their distinctively low ionization energy loss ( $dE/dx$ ) in the inner silicon tracker, a consequence of their reduced electric charge. In particular, the number of tracker measurements with low  $dE/dx$  values is used as discriminating variable with respect to SM processes. In the absence of significant deviations from the SM predictions, the study set exclusion limits at the 95% CL for FCPs with charges between  $e/3$  and  $e$ , excluding masses up to 640 GeV. These results represent the most stringent constraints to date on FCPs within the probed charge and mass ranges.

## 5 Displaced signatures

### 5.1 Displaced jet searches

A search for light LLPs decaying into displaced jets was conducted by CMS<sup>30</sup> using the first LHC Run-3 pp collisions at  $\sqrt{s} = 13.6$  TeV<sup>7</sup>, collected in 2022, corresponding to an integrated luminosity of  $34.7 \text{ fb}^{-1}$ . The search targets events with at least one light LLP of mass up to 60 GeV, decaying within the inner tracker. Decays into pairs of light quarks ( $d\bar{d}$ ), heavy quarks ( $b\bar{b}$ ), or tau leptons are considered. This Run-3 analysis relies on novel trigger and reconstruction techniques. New displaced-jet triggers increase the selection efficiency by almost an order of magnitude compared to the corresponding Run-2 searches. A new DV reconstruction algorithm is employed, especially improved for  $b\bar{b}$  final states. Two LLP taggers, based on graph neural networks, enhance the discrimination between signal and background events.

No significant excess over the expected background is observed, and upper limits are placed on the branching fraction of the Higgs boson decaying into light LLPs (see fig. 4 left). An improvement by up to a factor of 10 was achieved over Run-2 limits in the range of LLP masses and decay lengths considered. Notably, these are the first limits for this model with decays to displaced hadronic taus and decay lengths below 1 m.

Searches for displaced jets were carried out by ATLAS<sup>31</sup> as well, using  $140 \text{ fb}^{-1}$  of Run-2 data. In addition to the model presented above, these searches consider Higgs bosons produced via VBF and VH modes, and ALPs produced in association with a W or Z boson, and with a  $t\bar{t}$  pair.

### 5.2 Displaced lepton searches

CMS conducted a generic search for LLPs decaying into pairs of displaced leptons (electrons  $e$  or muons  $\mu$ )<sup>32</sup>, using Run-2 data corresponding to an integrated luminosity of  $118$  ( $113$ )  $\text{fb}^{-1}$  for the ee ( $e\mu$ ,  $\mu\mu$ ) final state(s).

Events with two leptons are selected, each having a transverse impact parameter between 0.01 and 10 cm. No requirement is made for the leptons to originate from a common DV. No significant excess over the SM background is observed in any of the channels. Upper limits are set on the production cross sections of LLPs decaying into leptons, providing constraints on various theoretical models: BSM Higgs bosons decaying to scalar LLPs,  $R$ -parity-violating SUSY, and gauge-mediated SUSY breaking (GMSB) models<sup>33</sup>.

ATLAS performed a similar search<sup>34</sup> on a larger data set, including the Run-2 data at  $\sqrt{s} = 13$  TeV and  $56.3 \text{ fb}^{-1}$  of Run-3 data at  $\sqrt{s} = 13.6$  TeV<sup>5</sup>. In the GMSB interpretation, tight limits on the slepton masses and lifetimes are set (see fig. 4 right).

### 5.3 Displaced dileptons with very low masses

Searches for very light LLPs (with masses below 1 GeV) decaying to fermion pairs were conducted by ATLAS<sup>35</sup> and CMS<sup>36</sup> with the Run-2 data, using different approaches. Both experiments

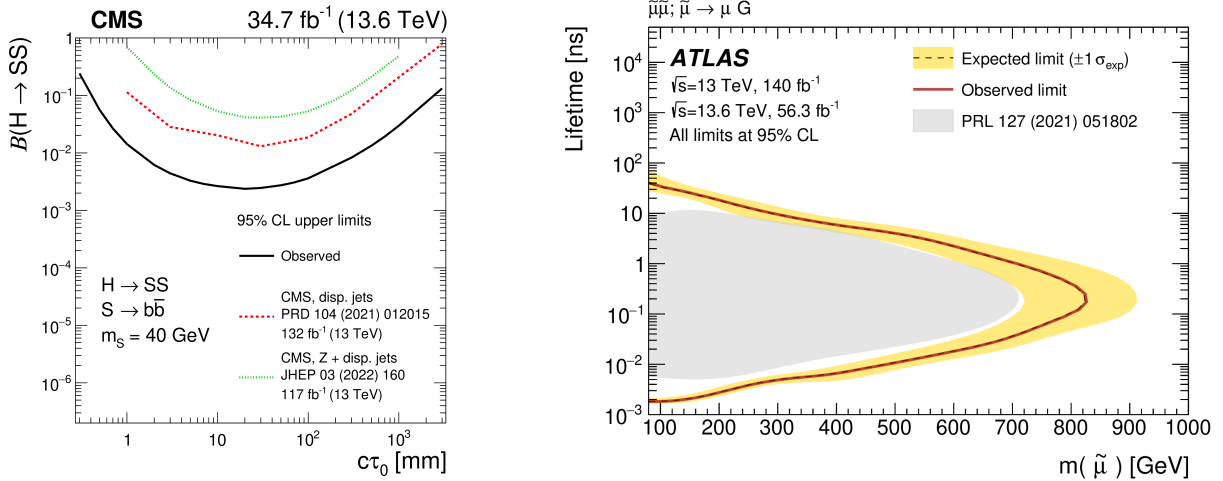


Figure 4 – Left: 95% CL observed upper limits on the branching fraction of the Higgs boson decay to scalar LLP  $S$  for the  $S \rightarrow b\bar{b}$  channel, for the Run-2 (red dashed line) and Run-3 (black solid line) CMS displaced-jet searches. Right: 95% CL exclusion contours on the smuon mass and lifetime, for smuon pair production in a GMSB model from the ATLAS Run-2 and Run-3 displaced-lepton searches.

provided results in the context of a Hidden Abelian Higgs Model (HAHM)<sup>37</sup>, where the Higgs boson decays to long-lived dark photons, which in turn decay to SM fermions.

The CMS search focused on muon pairs selected with a dedicated dimuon trigger stream (“scouting”)<sup>11</sup> with very low transverse momentum thresholds, recorded at high rate by retaining a reduced amount of information. This technique enables the exploration of regions of phase space characterized by dimuon masses as low as 500 MeV, and a significant displacement of the DV.

ATLAS searched for collimated muon pairs selected with dedicated MS-only triggers. Additionally, the search was extended to collimated electron and quark pairs, reconstructed as jets in the calorimeters with low ECAL-to-HCAL energy ratio<sup>8</sup>. The contribution of the latter channel allows ATLAS to explore LLP masses as low as 17 MeV.

## 6 Heavy neutral leptons

Heavy neutral leptons (HNLs)<sup>38</sup> are predicted in many BSM theories to explain the small masses of the SM neutrinos, e.g. via a seesaw mechanism. In addition, HNLs may explain the baryon asymmetry of the universe and provide viable DM candidates. In the searches presented below, HNLs are sterile and can only be produced via mixing with the SM neutrinos. Both HNLs of Dirac and Majorana nature are considered. The HNL lifetime,  $\tau_N$ , depends on its mass,  $m_N$ , and on its mixing probability with the SM neutrinos,  $|V_{\ell N}|^2$ , as  $\tau_N \sim m_N^{-5} |V_{\ell N}|^{-2}$ . Therefore, for  $m_N$  below about 20 GeV the HNL is long-lived and generates DVs in its decay.

At the LHC, HNL searches focus mostly on W boson decays (with leptonic or semi-leptonic final states)<sup>39,40,41,42,43</sup> or B meson decays<sup>44</sup>. A selection of the most recent HNL searches at CMS are reported below.

### 6.1 Long-lived HNLs in the semi-leptonic channel

CMS conducted searches for long-lived HNLs decaying into a jet and a charged lepton, considering both lepton-flavor conserving and violating processes, with the full Run-2 data set. The study explored HNL masses between 1 and 20 GeV, and lifetimes up to about 10 m. Two separate approaches were followed, both based on machine learning techniques, with partially overlapping parameter space sensitivity:

- displaced jet tagger<sup>41</sup>: deep neural network taking as input the displaced jet features;

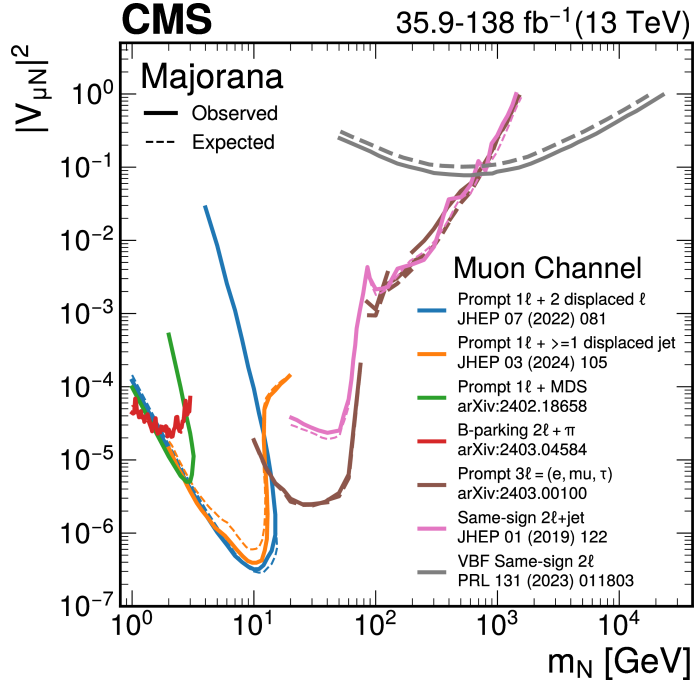


Figure 5 – Summary of searches at CMS for long-lived HNLs in a Type-I seesaw model. The observed limits at 95% CL on the mixing parameter  $|V_{\mu N}|^2$  as a function of the HNL mass  $m_N$  are shown for a Majorana HNL in the muon channel.

- particle flow net (PFN)<sup>42</sup>: deep-set neural network taking as input all the tracks from a DV, reconstructed from a lepton and hadron tracks.

## 6.2 Long-lived HNLs in B hadron decays

This CMS search<sup>44</sup> used  $41.6 \text{ fb}^{-1}$  of Run-2 data collected in 2018. It focuses on the decay chain  $B \rightarrow \ell_1 N$ , followed by  $N \rightarrow \ell_2 \pi$ , where  $\ell_1$  and  $\ell_2$  are either two muons or a muon and an electron. The study targets HNLs with  $m_N = 1\text{--}3 \text{ GeV}$  and decay lengths ranging from 0.01 to 100 m. A dedicated data stream (“data parking”) is employed to enhance the number of recorded events containing B mesons. A parametric neural network is used to select the HNL signal.

Upper limits on the mixing parameter  $|V_{\ell N}|^2$  as a function of  $m_N$  from all the CMS searches are shown in Fig. 5, for the case of a Majorana HNL. The complementarity of different final states, and of prompt and displaced topologies, can be appreciated.

## 7 Conclusions

The ATLAS and CMS experiments have developed a vast program to search for DSS and LLPs, employing a variety of innovative techniques to probe unexplored regions of parameter space. While no definitive signals have been observed to date, the constraints placed on theoretical models are invaluable in guiding future research directions, in view of the upcoming detector upgrades and increased LHC collision energies.

## References

1. G. Bertone, D. Hooper, J. Silk, *Phys. Rept.* **405**, 279-390 (2005).
2. E. Komatsu, *et al.*, *Astrophys. J. Suppl. Ser.* **192**, 18 (2011).
3. Planck Collaboration, *Astron. Astrophys.* **594**, A13 (2016).
4. ATLAS Collaboration, *JINST* **3**, S08003 (2008).

5. ATLAS Collaboration, *JINST* **19**, P05063 (2024).
6. CMS Collaboration, *JINST* **3**, S08004 (2008).
7. CMS Collaboration, *JINST* **19**, P05064 (2024).
8. ATLAS Collaboration, arXiv:2403.09292 [hep-ex] (2024).
9. CMS Collaboration, arXiv:2405.13778 [hep-ex] (2024).
10. CMS Collaboration, arXiv:2405.17605 [hep-ex] (2024).
11. CMS Collaboration, arXiv:2403.16134 [hep-ex] (2024).
12. D. Abercrombie, *et al.*, *Phys. Dark Univ.* **27**, 100371 (2020).
13. J. Andrea, *et al.*, *Phys. Rev. D* **84**, 074025 (2011).
14. ATLAS Collaboration, *J. High Energ. Phys.* **05**, 263 (2024).
15. CMS Collaboration, CMS-PAS-SUS-23-004 (2024).
16. CMS Collaboration, arXiv:2408.17336 [hep-ex] (2024).
17. ATLAS Collaboration, *J. High Energ. Phys.* **11**, 126 (2024).
18. R.E. Shrock, M. Suzuki, *Phys. Lett. B* **110**, 250 (1982).
19. D. Ghosh, *et al.*, *Phys. Lett. B* **725**, 344 (2013).
20. I. Brivio, *et al.*, *Eur. Phys. J. C* **77**, 8, 572 (2017).
21. ATLAS Collaboration, *Phys. Lett. B* **842**, 137963 (2023).
22. CMS Collaboration, *Eur. Phys. J. C* **83**, 933 (2023).
23. ATLAS Collaboration, ATLAS-CONF-2021-053 (2021).
24. G.D. Kribs, *et al.*, *J. High Energ. Phys.* **07**, 133 (2019).
25. ATLAS Collaboration, *J. High Energ. Phys.* **09**, 005 (2024).
26. S. Knapen, *et al.*, *J. High Energ. Phys.* **08**, 076 (2017).
27. CMS Collaboration, *Phys. Rev. Lett.* **133**, 191902 (2024).
28. B. Holdom, *Phys. Lett. B* **166**, 196-198 (1986).
29. CMS Collaboration, arXiv:2402.09932 [hep-ex] (2024).
30. CMS Collaboration, arXiv:2409.10806 [hep-ex] (2024).
31. ATLAS Collaboration, *Phys. Rev. Lett.* **133**, 161803 (2024).
32. CMS Collaboration, *Eur. Phys. J. C* **82**, 153 (2022).
33. M. Dine, W. Fischler, *Phys. Lett. B* **110**, 227 (1982).
34. ATLAS Collaboration, arXiv:2410.16835 [hep-ex] (2024).
35. ATLAS Collaboration, *J. High Energ. Phys.* **06**, 153 (2023).
36. CMS Collaboration, *J. High Energ. Phys.* **04**, 062 (2022).
37. D. Curtin, *et al.*, *J. High Energ. Phys.* **02**, 157 (2015).
38. Y. Cai, *et al.*, *Front. Phys.* **6**, 40 (2018).
39. ATLAS Collaboration, *Phys. Rev. Lett.* **131**, 061803 (2023).
40. CMS Collaboration, *J. High Energ. Phys.* **07**, 081 (2022).
41. CMS Collaboration, *J. High Energ. Phys.* **03**, 105 (2024).
42. CMS Collaboration, arXiv:2407.10717 [hep-ex] (2024).
43. CMS Collaboration, *Phys. Rev. D* **110**, 012004 (2024).
44. CMS Collaboration, *J. High Energ. Phys.* **06**, 183 (2024).